

See discussions, stats, and author profiles for this publication at: <https://www.researchgate.net/publication/233901870>

# Oxidation of Methane to Methanol with Hydrogen Peroxide Using Supported Gold-Palladium Alloy Nanoparticles

ARTICLE *in* ANGEWANDTE CHEMIE INTERNATIONAL EDITION · JANUARY 2013

Impact Factor: 11.26 · DOI: 10.1002/anie.201207717 · Source: PubMed

CITATIONS

23

READS

331

13 AUTHORS, INCLUDING:



**Nikolaos Dimitratos**

Cardiff University

100 PUBLICATIONS 3,006 CITATIONS

SEE PROFILE



**Jose Antonio Lopez-Sanchez**

University of Liverpool

75 PUBLICATIONS 2,266 CITATIONS

SEE PROFILE



**Albert Frederick Carley**

Cardiff University

244 PUBLICATIONS 9,189 CITATIONS

SEE PROFILE



**Damien M Murphy**

Cardiff University

135 PUBLICATIONS 2,546 CITATIONS

SEE PROFILE

# Oxidation of Methane to Methanol with Hydrogen Peroxide Using Supported Gold–Palladium Alloy Nanoparticles\*\*

Mohd Hasbi Ab Rahim, Michael M. Forde, Robert L. Jenkins, Ceri Hammond, Qian He, Nikolaos Dimitratos, Jose Antonio Lopez-Sanchez, Albert F. Carley, Stuart H. Taylor, David J. Willock, Damien M. Murphy, Christopher J. Kiely, and Graham J. Hutchings\*

The direct conversion of methane to methanol remains a key challenge. The current commercial production of methanol from methane has been fine-tuned over many decades of operation and gives a high selectivity for the formation of methanol, but involves a high energy input two-stage process. Direct conversion of methane to methanol in a single step would clearly provide many advantages.<sup>[1]</sup> Catalysts identified that operate at high temperature can give a high methanol selectivity at low conversion.<sup>[2]</sup> Using milder reaction conditions catalysts do not give closed catalytic cycles.<sup>[3–12]</sup> Recently we have shown that CuFe-ZSM-5 is an effective catalyst for the conversion of methane to methanol with a closed catalytic cycle when H<sub>2</sub>O<sub>2</sub> was used as an oxidant.<sup>[13]</sup> This has prompted us to investigate the use of other catalysts with this oxidant. We have previously shown that supported Au-Pd nanoparticles are highly effective catalysts for the direct synthesis of H<sub>2</sub>O<sub>2</sub>,<sup>[14]</sup> the oxidation of alcohols,<sup>[15]</sup> and the oxidation of primary C–H bonds in toluene.<sup>[16]</sup> We consider that all these reactions are linked by the formation of a hydroperoxy intermediate from dioxygen. We considered that a hydroperoxy species may be effective for the oxidation, since it is known that H<sub>2</sub>O<sub>2</sub> or *tert*-butyl hydroperoxide (TBHP) have been used to oxidize methane.<sup>[17–19]</sup> In view of this we have used hydrogen peroxide as oxidant and here we show that Au-Pd supported nanoparticles are active for the oxidation of methane, giving a high selectivity for the formation of methanol, especially when the reaction is carried out in the presence of hydrogen peroxide generated *in situ* from hydrogen and oxygen.

In a typical reaction, the oxidation of methane is performed in liquid phase using an autoclave reactor with water as solvent and H<sub>2</sub>O<sub>2</sub> as oxidant. Initially, we investigated the activity of supported Au-Pd/TiO<sub>2</sub> prepared by sol immobilization<sup>[16]</sup> but found high H<sub>2</sub>O<sub>2</sub> decomposition (Table 1, entry 1). We considered that the high H<sub>2</sub>O<sub>2</sub> decomposition rate which was facilitated by the small size and metallic oxidation state of the AuPd nanoparticles. Therefore, we used Au-Pd catalysts prepared by incipient wetness (IW), as they have been shown to be effective in the direct synthesis of H<sub>2</sub>O<sub>2</sub> with low decomposition/hydrogenation rates.<sup>[14]</sup> Using 1 wt % Au-Pd/TiO<sub>2</sub> (IW) the turnover frequency (TOF) for methane oxidation was increased by a factor of two and about 58 % of the oxidant remained after reaction, as opposed to the complete decomposition of H<sub>2</sub>O<sub>2</sub> that was observed with the sol immobilization catalyst (Table 1, entries 1 and 2). The selectivity to methanol was lower in the case of the IW catalyst, this being due to a higher selectivity to methyl hydroperoxide.

Encouraged by these results, we examined the effect of temperature on the catalytic activity (Table 1, entries 3–5) since it has been reported that HAuCl<sub>4</sub> (and other metal chlorides) can be very active for the aqueous phase oxidation of methane using hydrogen peroxide at 90 °C.<sup>[17]</sup> HCOOH and CO<sub>2</sub> were the main products of the high temperature homogeneous oxidation,<sup>[20]</sup> accompanied by metal mineralization, whilst there was a marked reduction in catalytic activity at 50 °C (see Table S1 in the Supporting Information). For the heterogeneously catalyzed reaction, as the temperature was increased the catalytic productivity improved markedly. The maximum TOF (ca. 25 h<sup>–1</sup>) and the highest methanol selectivity under these conditions (19 %), was achieved at 90 °C (Table 1, entry 3). Remarkably, methanol was stable at 90 °C under our reaction conditions, but we noted that methyl hydroperoxide was the major reaction product in all cases. Süss-Fink and co-workers<sup>[21]</sup> have shown that methyl hydroperoxide is transformed to formaldehyde and formic acid at temperatures above 40 °C in the absence of a catalyst. However, at the temperatures we employed (30–90 °C) these particular products were not observed, suggesting that the formation of methyl hydroperoxide and methanol is due to the presence of the Au-Pd catalyst.

We reasoned that the low methanol selectivity could be linked to the low metal loading (7.24 × 10<sup>–7</sup> mol) employed in these reactions and therefore tested 2.5 wt % Au–2.5 wt % Pd/TiO<sub>2</sub> (IW), a material which has been well characterized in a number of previous publications and so the results will not

[\*] Dr. M. H. Ab Rahim,<sup>[†]</sup> Dr. M. M. Forde, Dr. R. L. Jenkins, Dr. C. Hammond, Dr. N. Dimitratos, Dr. J. A. Lopez-Sanchez, Dr. A. F. Carley, Dr. S. H. Taylor, Dr. D. J. Willock, Dr. D. M. Murphy, Prof. G. J. Hutchings  
Cardiff Catalysis Institute, Cardiff University  
Main Building, Park Place CF103AT Cardiff (UK)  
E-mail: hutch@cardiff.ac.uk

Dr. Q. He, Prof. C. J. Kiely  
Department of Materials Science and Engineering  
Leigh University  
5 East Packer Avenue, Bethlehem, PA 18015-3195 (USA)

[†] Current address: Faculty of Industrial Sciences & Technology  
University Malaysia Pahang  
Lebuhraya Tun Razak, 26300, Kuantan, Pahang (Malaysia)

[\*\*] This work formed part of the Methane Challenge. The Dow Chemical Company is thanked for their financial support.

Supporting information for this article is available on the WWW under <http://dx.doi.org/10.1002/anie.201207717>.

**Table 1:** Comparative catalytic activity of various Au-based catalysts for the liquid-phase oxidation of methane, with hydrogen peroxide either 1) added as co-reactant or 2) generated in situ from a H<sub>2</sub>/O<sub>2</sub> mixture under mild conditions.<sup>[a]</sup>

Entry	Catalyst	Metal <sup>[b]</sup> [wt %]	T [°C]	Oxidant	Products [μmol]				Oxy. sel. <sup>[e]</sup> [%]	CH <sub>3</sub> OH sel. <sup>[f]</sup> [%]	Total prod. <sup>[g]</sup> [mol kg <sub>cat</sub> <sup>-1</sup> h <sup>-1</sup> ]	TOF <sup>[h]</sup> [h <sup>-1</sup> ]	H <sub>2</sub> O <sub>2</sub> <sup>[i]</sup> [μmol]
					CH <sub>3</sub> OH <sup>[c]</sup>	HCOOH <sup>[c]</sup>	MeOOH <sup>[c]</sup>	CO <sub>2</sub> <sup>[d]</sup> [g]					
1	AuPd/TiO <sub>2</sub> (sol im.)	1.0	50	H <sub>2</sub> O <sub>2</sub>	0.60	0	0	0.41	59.4	59.4	0.10	2.79	< 15
2	AuPd/TiO <sub>2</sub>	1.0	50	H <sub>2</sub> O <sub>2</sub>	0.30	0	1.82	0.36	85.4	12.1	0.50	6.85	2894
3	AuPd/TiO <sub>2</sub>	1.0	90	H <sub>2</sub> O <sub>2</sub>	1.84	0	6.39	1.08	88.4	19.8	1.86	25.72	278
4	AuPd/TiO <sub>2</sub>	1.0	70	H <sub>2</sub> O <sub>2</sub>	0.66	0	3.90	0.47	88.9	12.9	1.03	14.17	1595
5	AuPd/TiO <sub>2</sub>	1.0	30	H <sub>2</sub> O <sub>2</sub>	0.19	0	1.09	0.28	82.6	12.2	0.31	4.28	3988
6	AuPd/TiO <sub>2</sub>	5.0	50	H <sub>2</sub> O <sub>2</sub>	1.89	0	1.57	0.37	90.3	49.3	0.28	0.77	383
7	AuPd/TiO <sub>2</sub>	5.0	2	H <sub>2</sub> O <sub>2</sub>	1.31	0	1.40	0.19	93.4	45.2	0.21	0.58	4471
8	Au/ TiO <sub>2</sub> + Pd/ TiO <sub>2</sub> *	5.0	50	H <sub>2</sub> /O <sub>2</sub>	0.12	0	0	0.54	18.2	18.2	0.009	0.024	33
9	Au/ TiO <sub>2</sub> + Pd/ TiO <sub>2</sub> **	5.0	50	H <sub>2</sub> /O <sub>2</sub>	0.81	0	0	0.58	58.3	58.3	0.059	0.162	21
10	AuPd/TiO <sub>2</sub>	5.0	50	H <sub>2</sub> /O <sub>2</sub>	1.31	0	0.29	0.32	83.3	68.2	0.116	0.320	56
11	AuPd/TiO <sub>2</sub>	5.0	2	H <sub>2</sub> /O <sub>2</sub>	0.26	0	0.47	0.15	83.0	29.5	0.053	0.146	124
12	AuPd/TiO <sub>2</sub>	5.0	70	H <sub>2</sub> /O <sub>2</sub>	0.81	0	0.1	0.11	89.2	79.4	0.059	0.164	29
13	AuPd/TiO <sub>2</sub>	5.0	50	NADH/ O <sub>2</sub>	4.48	0	0	0.54	89.2	89.2	0.081	0.224	n.d.

[a] Typical reaction conditions: time: 30 minutes, pressure of CH<sub>4</sub>: 30.5 bar, stirring rate: 1500 rpm, entries 1–5 catalyst:  $7.24 \times 10^{-7}$  mol of metals equal to 10 mg of solid catalysts, entries 6–13 catalyst:  $1.0 \times 10^{-5}$  mol of metals equal to 28 mg of solid catalysts, volume: 10 mL of H<sub>2</sub>O. [H<sub>2</sub>O<sub>2</sub>]: 0.5 M, H<sub>2</sub>/O<sub>2</sub> gases mixture: 0.86% H<sub>2</sub>/1.72% O<sub>2</sub>/75.86% CH<sub>4</sub>/21.55% N<sub>2</sub>. \*Reaction of a physical mixture comprising 2.5 wt % Au/TiO<sub>2</sub> and 2.5 wt % Pd/TiO<sub>2</sub> at a 1:1 weight ratio for 28 mg of the total catalyst. \*\*Reaction of a physical mixture comprising 2.5 wt % Au/TiO<sub>2</sub> and 2.5 wt % Pd/TiO<sub>2</sub> at a 1:1 molar metal ratio for 28 mg of the total catalyst. All solid catalysts have been prepared by incipient wetness and calcined at 400 °C for 3 h in static air, except for entry 1. n.d. = not determined. [b] The weight ratio Au: Pd in a bimetallic catalyst is 1:1. [c] Analyzed by <sup>1</sup>H NMR spectroscopy with 1% TMS in CDCl<sub>3</sub> internal standard. [d] Analyzed by a gas chromatography/flame ionization detection. Values obtained from a CO<sub>2</sub> calibration curve. [e] Calculated as moles(oxygenates)/moles(total products) 100. [f] Calculated as moles(MeOH)/moles(total products) 100. [g] Calculated as moles(products)/weight(catalyst)/time. [h] Calculated as moles(products)/moles(metal catalyst)/time. [i] Remaining H<sub>2</sub>O<sub>2</sub> assayed by Ce<sup>IV</sup>(aq.) titration. sol im.: sol immobilization; oxy.: oxygenate; sel.: selectivity, and prod.: productivity.

be repeated here.<sup>[14,15]</sup> For completeness, detailed scanning transmission electron microscopy characterization of the 1 wt % Au-Pd/TiO<sub>2</sub> (IW) catalyst has also been performed as shown in Figure 1. Many of the metal particles were found to be in the 5–20 nm size range, (Figure 1a,b), and were confirmed to be AuPd alloys that were consistently enriched in Au compared to the nominal composition (Figure 1c). Furthermore a Pd-rich shell/Au-rich core morphology would be detected in many of these 5–20 nm particles by virtue of their characteristic z-contrast in the high-angle annular dark-field (HAADF) imaging mode (Figure 1b). Higher magnification HAADF images also showed the existence of a significant population of 1–2 nm particles and subnanometer clusters (Figure 1d,e), which X-ray energy dispersive spectroscopy (XEDS) analysis (Figure 1f) showed to be Pd-rich in character. Furthermore, some occasional 100–200 nm particles which were Au-rich could also be found when the sample was examined by SEM (Figure S1), indicating that the initial dispersion of the Au precursor was not perfect. The particle size distribution and characteristic particle size/composition trend were found to be similar for both the 0.5 wt % Au-0.5 wt % Pd/TiO<sub>2</sub> (IW) and the 2.5 wt % Au-2.5 wt % Pd/TiO<sub>2</sub> (IW) catalyst materials, with the only significant difference being the obviously higher overall metal loading in the latter sample.

The 5 wt % metal catalyst gives a higher methanol selectivity than that observed with the 1 wt % Au-Pd/TiO<sub>2</sub> (IW) catalyst (i.e. 49% versus 14%, Table 1, entries 6 versus 2), but a similar overall oxygenate selectivity. The overall catalyst productivity is lower for the 5 wt % metal-loaded catalyst and this is linked to the high H<sub>2</sub>O<sub>2</sub> decomposition rate, as is the case for the sol immobilization catalyst. Hence we investigated the 5 wt % catalyst at a lower temperature (2 °C) and observed methane activation with 93% oxygenate selectivity (45% to methanol), low H<sub>2</sub>O<sub>2</sub> usage (about 90% left after reaction) and a similar rate to higher temperature reactions (Table 1, entry 7). Changing the weight percent ratio of Au: Pd alters the conversion and product distribution (Table S2).

As titania is well-known for activating hydrogen peroxide to produce surface-stabilized peroxo- or hydroperoxo species (TiO<sub>2</sub>-O<sub>2</sub><sup>-</sup> and Ti-OOH),<sup>[22]</sup> we performed experiments using TiO<sub>2</sub> as catalyst. No products were observed indicating that TiO<sub>2</sub> cannot oxidize CH<sub>4</sub> in the absence of the AuPd component of the catalyst. (Table S2). However, the identity of the support may affect the conversion and product distribution for AuPd catalysts (Table S3). In agreement with previously reported data,<sup>[13,18]</sup> higher CH<sub>4</sub> pressures and increasing the initial concentration of H<sub>2</sub>O<sub>2</sub> have the clear effect of increasing the total oxygenates produced with no

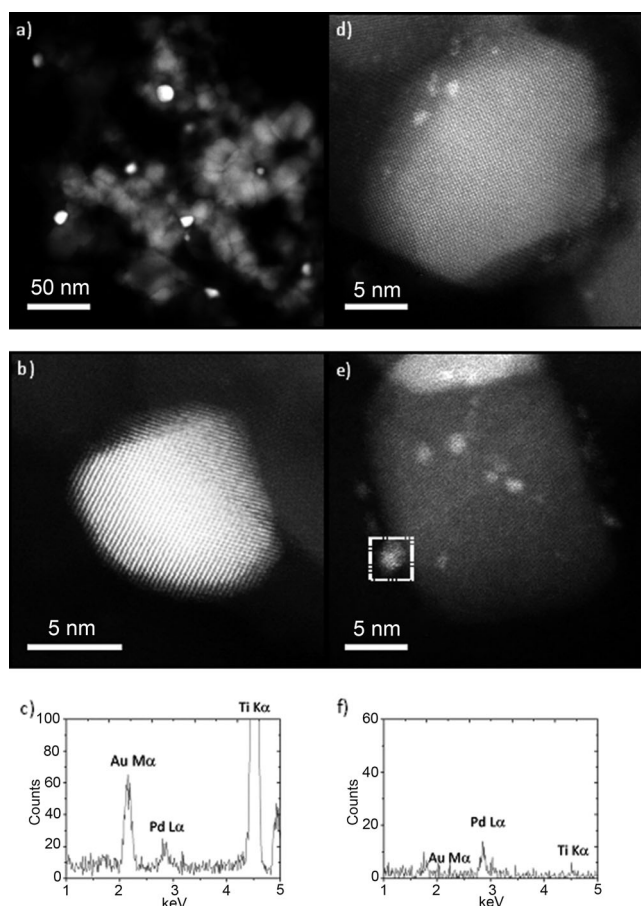


**Figure 1.** Representative scanning transmission electron microscopy (STEM) HAADF images and corresponding STEM-XEDS spectra from the 1 wt% AuPd/TiO<sub>2</sub> (IW) sample. a,b) Low and higher magnification HAADF images showing metal particles in the 5–20 nm size range. c) The XEDS spectrum obtained from the 10 nm particle shown in (b) which indicates that it is a Au-Pd alloy that is enriched in Au compared to the nominal composition. A distinct Au-rich core/Pd-rich shell morphology can also be deduced from image (b) as the particle exhibits significantly fainter contrast at its extremity. d,e) Even higher magnification HAADF images showing a significant population of 1–2 nm particles and subnanometer clusters co-existing on the TiO<sub>2</sub> support surface. f) The XEDS spectrum of the particle highlighted in (e) suggests that these smaller species are very Pd-rich.

appreciable loss in methanol selectivity over the ranges studied (Figures S2 and S3). Furthermore, prolonging the reaction time at 50 °C increased the methanol formation to give a maximum selectivity of about 50% (Figure 2a). We also noted that methyl hydroperoxide, recently identified in our work with ZSM-5 as the primary reaction product of methane oxidation,<sup>[13]</sup> is also present in the Au-Pd system. This time-on-line study clearly demonstrates that methyl hydroperoxide is the primary reaction product being subsequently transformed to methanol and CO<sub>2</sub> in the presence of the catalyst, but significantly without the generation of formic acid at the concentrations that we have employed. Hence these data support the hypothesis that both the oxidation of methane and the subsequent oxidation of the primary reaction product are mediated by the Au-Pd surface.

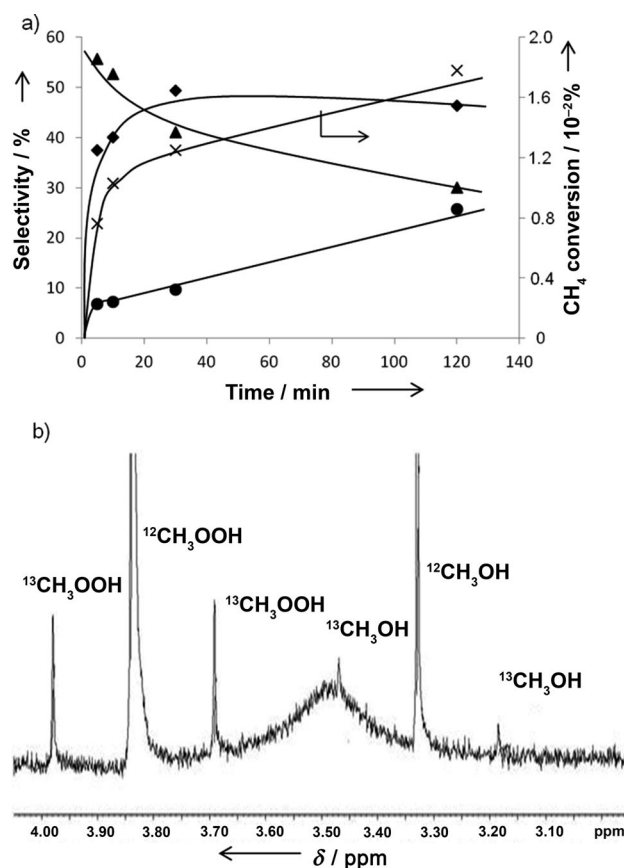


**Figure 2.** a) Time-on-line plot of methane oxidation with addition of H<sub>2</sub>O<sub>2</sub> in the presence of a 1 wt% AuPd/TiO<sub>2</sub> (IW) catalyst. Key: ▲ selectivity to methyl hydroperoxide, ◆ selectivity to methanol, ● selectivity to carbon dioxide, x methane conversion. Reaction conditions:  $P_{(\text{CH}_4)} = 30.5$  bar,  $[\text{H}_2\text{O}_2] = 0.5$  M,  $T = 50^\circ\text{C}$ , stirring rate = 1500 rpm, and catalyst mass = 10 mg. b) <sup>1</sup>H NMR spectrum of the reaction filtrate collected when using a solution initially spiked with <sup>13</sup>CH<sub>3</sub>OOH in a typical reaction using 5 wt% Au-Pd/TiO<sub>2</sub> (IW) and pure <sup>12</sup>CH<sub>4</sub>.

We considered that it was important to establish the reaction pathway and probe mechanistic aspects of this catalyzed reaction. To this end, we first synthesized <sup>13</sup>C-oxygenated products using <sup>13</sup>CH<sub>4</sub> to verify that all of the observed products were derived from methane. We also introduced a known amount of the isotopically labelled <sup>13</sup>CH<sub>3</sub>OOH into a typical reaction using a 5 wt% Au-Pd/TiO<sub>2</sub> (IW) catalyst and a pure <sup>12</sup>CH<sub>4</sub> gas feed. The <sup>1</sup>H NMR analysis of the post-reaction mixture showed the presence of <sup>13</sup>CH<sub>3</sub>OH and <sup>12</sup>CH<sub>3</sub>OH (Figure 2b). In the absence of the catalyst, however, no <sup>13</sup>CH<sub>3</sub>OH was observed. As pure <sup>12</sup>CH<sub>4</sub> was used in the second step, we confirmed that <sup>13</sup>CH<sub>3</sub>OOH is transformed into <sup>13</sup>CH<sub>3</sub>OH by the Au-Pd catalyst as the reaction proceeds. Additionally, when methanol is used as a substrate only 29% is oxidized at 50 °C, mainly to CO<sub>2</sub>, but we observe that formaldehyde and formic acid undergo facile oxidation to CO<sub>2</sub> (Table S4).

To investigate the nature of the oxidation we carried out electron paramagnetic resonance (EPR) studies under catalytic reaction conditions. 5,5'-Dimethyl-1-pyrroline-*N*-oxide (DMPO), was selected as a radical trap as it is routinely used

to detect a number of radical species which may be produced (i.e.  $\cdot\text{CH}_3$ ,  $\cdot\text{OCH}_3$ ,  $\cdot\text{OH}$ ,  $\cdot\text{OOH}$ ,  $\text{O}_2^-$ ). Our studies showed that both  $\cdot\text{CH}_3$  and  $\cdot\text{OH}$  were formed during the reaction (Figure 3). We could not detect any other oxygen-based radicals, but they cannot be totally excluded because of other

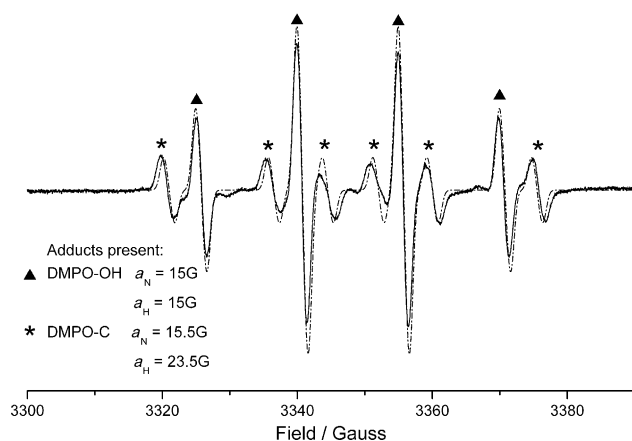


**Figure 3.** Electron paramagnetic resonance (EPR) spectrum showing radical species detected during the reaction of methane and  $\text{H}_2\text{O}_2$  over a 5 wt% Au-Pd/TiO<sub>2</sub> (1W) catalyst with DMPO added to the reaction mixture as the radical trapping agent. Key: black solid line: experimental signal, black dashed line: combined simulated signal for both  $\cdot\text{OH}$  and  $\cdot\text{CH}_3$  adducts, triangles: DMPO-OH adduct, and stars: DMPO- $\text{CH}_3$  adduct ( $a_N$  and  $a_H$  are the hyperfine coupling constants of the N and H atoms).

factors relating to the experimental procedure employed, especially since we have shown previously that Au-Pd/TiO<sub>2</sub> catalysts produce superoxide species associated with the titania support when exposed to organic peroxides.<sup>[23]</sup> Consequently, we consider that the methane oxidation mechanism for supported Au-Pd nanoparticles involves  $\cdot\text{CH}_3$  and this is in contrast to the reaction mechanism previously proposed for methane oxidation using CuFe-ZSM-5 where  $\cdot\text{CH}_3$  radicals are not observed.<sup>[13]</sup> The termination reaction of methyl radicals with hydrogen peroxide or  $\cdot\text{OH}$  would produce methane or form methanol, respectively. Dissolved  $\text{O}_2$ , originating from hydrogen peroxide decomposition on the catalyst surface, or a surface bound  $\cdot\text{OOH}$  may interact with methyl radicals to form  $\text{CH}_3\text{OO}\cdot$ . We favor the latter explanation due to the observation of methyl hydroperoxide as the primary reaction product.

In subsequent experiments we considered that using a hydroperoxy species generated in situ from molecular oxygen may be beneficial for the reaction. As the 5 wt% Au-Pd/TiO<sub>2</sub> catalyst is very efficient for the synthesis of  $\text{H}_2\text{O}_2$ ,<sup>[24]</sup> we performed reactions using  $\text{CH}_4$ ,  $\text{H}_2$ , and  $\text{O}_2$  diluted with  $\text{N}_2$  (0.86 % of  $\text{H}_2$  and 1.72 % of  $\text{O}_2$  in the reactor gas feed) for the concurrent synthesis of in situ hydrogen peroxide and eventual formation of methanol. Physical mixtures of Au/TiO<sub>2</sub> and Pd/TiO<sub>2</sub>, either in equimolar metal amounts or the same metal weight percent, gave inferior activity and selectivity compared to the titania-supported Au-

Pd alloy nanoparticles (Table 1, entries 8–10). This observation is in line with synergistic effects of Au-Pd alloys obtained with other substrates.<sup>[14–16,23,24]</sup>

More importantly, a similar productivity, but with improved methanol selectivity, was observed when using the in situ generated  $\text{H}_2\text{O}_2$  as compared to the experiments performed with pre-formed  $\text{H}_2\text{O}_2$  (0.5 M; Table 1, entries 6 and 10). We considered that based on the gas-phase composition, the theoretical maximum amount of  $\text{H}_2\text{O}_2$  which can be formed under these conditions is about 250  $\mu\text{mol}$ . Indeed, the in situ method leads to a three-fold increase in reactivity as compared to the reaction performed using low amounts of preformed  $\text{H}_2\text{O}_2$  (Table 1, entry 10, and Figure S3). Thus it is clear that the use of oxygen is improved by adopting an in situ capture approach. It has been previously shown that efficient  $\text{H}_2\text{O}_2$  synthesis can be performed at 2 °C with a similar catalyst,<sup>[14,24]</sup> therefore we investigated the oxidation of methane by using in situ generated hydrogen peroxide at this temperature. The data (Table 1, entry 11) demonstrate that Au-Pd supported nanoparticles generate the hydroperoxy species, as evidenced by the detection of  $\text{H}_2\text{O}_2$  at the end of the reaction, and also activate methane under these very mild conditions. In addition, a higher selectivity for the formation of methanol (about 80 %) was achieved by performing the reaction at 70 °C, but the overall oxygenate productivity did not improve (Table 1, entry 12). Increasing the  $\text{H}_2$  and  $\text{O}_2$  pressure, which should improve the amount of  $\text{H}_2\text{O}_2$  synthesized,<sup>[25,26]</sup> leads to an increase of methane conversion and methanol formation (Table S5). Prolonging the reaction time from 0.5 to 4 h is accompanied by an enhancement of methanol formation from 0.24 to 2.02  $\mu\text{mol}$ , but longer reaction times also facilitates the conversion of methanol to  $\text{CO}_2$  (Table S6). These results demonstrate that there is the possibility of increasing the yield of methanol if the contact time and reaction conditions are further optimized.

We also used a soluble co-reductant, reduced nicotinamide adenine dinucleotide (NADH), with the AuPd catalyst, and  $\text{O}_2$  to probe the efficiency of the  $-\text{H}$  use (Table 1, entry 13). The total amount of products observed was about half the amount of NADH added at the start of the experiment. This data suggest that the system can also achieve a high efficiency of  $-\text{H}$  use and that a water soluble  $-\text{H}$  donor may be used in place of gas-phase  $\text{H}_2$ .

In conclusion, we have shown that supported Au-Pd catalysts can be effective for the oxidation of methane to methanol using hydrogen peroxide as oxidant. The primary product is methyl hydroperoxide which we consider is formed from the reaction of  $\text{H}_2\text{O}_2$  with  $\cdot\text{CH}_3$ .

Received: September 24, 2012

Revised: November 23, 2012

Published online: December 11, 2012

**Keywords:** alloys · gold · methane · oxidation · palladium

[1] H. D. Gesser, N. R. Hunter, C. B. Prakash, *Chem. Rev.* **1985**, 85, 235–244.



- [2] R. Pitchai, K. Klier, *Catal. Rev. Sci. Eng.* **1986**, 28, 13–88.
- [3] A. E. Shilov, G. B. Shul'pin, *Chem. Rev.* **1997**, 97, 2879–2932.
- [4] R. H. Crabtree, *Chem. Rev.* **1995**, 95, 987–1007.
- [5] J. H. Lunsford, *Catal. Today* **2000**, 63, 165–174.
- [6] K. Otsuka, Y. Wang, *Appl. Catal. A* **2001**, 222, 145–161.
- [7] D. Wolf, *Angew. Chem.* **1998**, 110, 3545–3547; *Angew. Chem. Int. Ed.* **1998**, 37, 3351–3353.
- [8] L. C. Kao, A. C. Hutson, A. Sen, *J. Am. Chem. Soc.* **1991**, 113, 700–701.
- [9] R. A. Periana, D. J. Taube, E. R. Evitt, D. G. Löffler, P. R. Wentrick, G. Voss, T. Masuda, *Science* **1993**, 259, 340–343.
- [10] R. A. Periana, D. J. Taube, S. Gamble, H. Taube, T. Satoh, H. Fujii, *Science* **1998**, 280, 560–564.
- [11] R. Palkovits, M. Antonietti, P. Kuhn, A. Thomas, F. Schüth, *Angew. Chem.* **2009**, 121, 7042–7045; *Angew. Chem. Int. Ed.* **2009**, 48, 6909–6912.
- [12] A. B. Sorokin, E. V. Kudrik, D. Bouchu, *Chem. Commun.* **2008**, 2562–2564.
- [13] C. Hammond, M. M. Forde, M. H. Ab Rahim, A. Thetford, Q. He, R. L. Jenkins, N. Dimitratos, J. A. Lopez-Sanchez, N. F. Dummer, D. M. Murphy, A. F. Carley, S. H. Taylor, D. J. Willock, E. E. Stangland, J. Kang, H. Hagen, C. J. Kiely, G. J. Hutchings, *Angew. Chem.* **2012**, 124, 5219–5223; *Angew. Chem. Int. Ed.* **2012**, 51, 5129–5133.
- [14] J. K. Edwards, B. E. Solsona, P. Landon, A. F. Carley, A. Herzing, C. J. Kiely, G. J. Hutchings, *J. Catal.* **2005**, 236, 69–79.
- [15] D. I. Enache, J. K. Edwards, P. Landon, B. Solsona, A. F. Carley, A. A. Herzing, M. Watanabe, C. J. Kiely, D. W. Knight, G. J. Hutchings, *Science* **2009**, 311, 362–365.
- [16] L. Kesavan, R. Tiruvalam, M. H. A. Rahim, M. I. Saiman, D. I. Enache, R. L. Jenkins, N. Dimitratos, J. A. L. Sanchez, S. H. Taylor, D. W. Knight, C. J. Kiely, G. J. Hutchings, *Science* **2006**, 331, 195–199.
- [17] Y. Qiang, D. Weiping, Q. Zhang, Y. Wang, *Adv. Synth. Catal.* **2007**, 349, 1199–1209.
- [18] G. B. Shul'pin, T. Sooknoi, V. Romakh, G. Süss-Fink, L. S. Shul'pina, *Tetrahedron Lett.* **2006**, 47, 3071–3075.
- [19] R. Raja, P. Ratnasamy, *Appl. Catal. A* **1997**, 158, L7–L15.
- [20] For the homogeneous oxidation reactions the total amount of metal used equaled the total amount of metal used in the heterogeneous oxidation reactions with 2.5wt % Au-2.5wt % Pd/TiO<sub>2</sub> catalyst,  $1 \times 10^{-5}$  moles. These experiments were performed to compare the possible catalytic activity of the homogeneous Au or Pd metals under our typical reaction conditions.
- [21] G. Süss-Fink, G. V. Nizova, S. Stanislas, G. B. Shul'pin, *J. Mol. Catal. A* **1998**, 130, 163–170.
- [22] F. Bonino, A. Damin, G. Ricchiardi, M. Ricci, G. Spanò, R. D'Aloisio, A. Zecchina, C. Lamberti, C. Prestipino, S. Bordiga, *J. Phys. Chem. B* **2004**, 108, 3573–3583.
- [23] M. I. Bin Saiman, G. L. Brett, R. Tiruvalam, M. M. Forde, K. Sharples, A. Thetford, R. L. Jenkins, N. Dimitratos, J. A. Lopez-Sanchez, D. M. Murphy, D. Bethell, D. J. Willock, S. H. Taylor, D. W. Knight, C. J. Kiely, G. J. Hutchings, *Angew. Chem.* **2012**, 124, 6083–6087; *Angew. Chem. Int. Ed.* **2012**, 51, 5981–5985.
- [24] J. K. Edwards, B. Solsona, E. Ntainjua, A. F. Carley, A. A. Herzing, C. J. Kiely, G. J. Hutchings, *Science* **2009**, 323, 1037–1041.
- [25] M. Piccinini, E. Ntainjua, J. K. Edwards, A. F. Carley, J. A. Moulijn, G. J. Hutchings, *Phys. Chem. Chem. Phys.* **2010**, 12, 2488–2492.
- [26] M. Piccinini, E. Ntainjua, J. K. Edwards, A. F. Carley, J. A. Moulijn, G. J. Hutchings, *Catal. Sci. Technol.* **2012**, 2, 1908–1913.